Factors Influencing Staging during Anion-Exchange Intercalation into $[LiAl_2(OH)_6]X{\cdot}mH_2O$ ($X = Cl^-$, Br^-, NO_3^-)

Gareth R. Williams and Dermot O'Hare*

Chemistry Research Laboratory, University of Oxford, Mansfield Road, Oxford, OX1 3TA, U.K.

Received February 14, 2005. Revised Manuscript Received March 24, 2005

A variety of organic carboxylates and phosphonates have been intercalated into the hexagonal and rhombohedral polymorphs of $[LiAl_2(OH)_6]X{\cdot}mH_2O$, with $X = Cl^-$, Br^-, and NO_3^-. The two classes of polytype differ in the stacking sequence of the layers (*aba* and *abca*, respectively). Both the initial interlayer anion and the stacking sequence of the host are seen to have a profound effect on whether anion-exchange intercalation reactions occur in a one-step direct transformation from the host to the first-stage intercalated product, or whether the reaction proceeds via a second-stage intermediate. Generally, staging is much more prevalent in the hexagonal system, and with the harder to replace Cl^- and Br^- anions. Overall, the occurrence of staging appears to be strongly correlated with the rate of anion exchange in these materials.

Introduction

Intercalation has long been of interest to scientists because it allows the electronic, magnetic, and optical properties of solid host matrixes to be modified with minimal change to the structure.[1−3] Layered double hydroxides (LDHs) are attractive hosts for intercalation reactions because they consist of positively charged layers and charge-balancing anions in the interlayer regions. These anions can be exchanged for other guest anions. LDHs typically have the formula $[M_2^{2+}M^{3+}(OH)_6]^+X_{1/n}^{n-}{\cdot}mH_2O$. They occur in two classes of polytype, which differ in the way in which the layers stack. The rhombohedral form has an *abca* stacking sequence and the hexagonal form an *aba* stacking sequence.

$[LiAl_2(OH)_6]X{\cdot}mH_2O$ (LiAl-X) is unique among LDHs in that it is the only stable LDH to contain +1 and +3 metal centers: all other LDHs contain differing ratios of di- and trivalent metal cations. Also, the cation ordering present in LiAl−Cl is unusual in LDH chemistry.[4] The two types of metal cations in the layers tend to be disordered: although short-range order has been seen by EXAFS experiments, long-range order is rare. The extreme long-range order of the LiAl−X systems results from the synthesis method. LDHs are usually synthesized via a coprecipitation route in which a solution of the M^{2+}/M^{3+} cations is added to a basic solution of the desired interlayer anion. In contrast, LiAl−X is synthesized from the reaction of LiX with $Al(OH)_3$. The Li^+ cations occupy the remaining octahedral sites in the γ-$Al(OH)_3$ layers in an ordered fashion. The polymorph of $Al(OH)_3$ used determines the stacking sequence of the layers in the final LDH. Gibbsite gives the hexagonal form, whereas reaction with bayerite or nordstrandite produces the rhombohedral polymorph.[5] This arises as a result of differences in the stacking of the layers between the $Al(OH)_3$ polymorphs.

LDHs possess a number of desirable properties. The hexagonal form of $[LiAl_2(OH)_6]Cl{\cdot}H_2O$ (h-LiAl−Cl) has been shown to exhibit shape-selective ion exchange,[6−8] and certain LDHs are known to have catalytic properties.[3,9] Some contemporary applications of LDHs have recently been reviewed by O'Hare and other authors.[10−12]

The mechanisms by which intercalation occurs in layered hosts are currently not well understood. It is thought that the reaction is initiated at crystal defects on either the basal plane surface or edge plane of a host crystallite, which means differences in reactivity are often observed between batches of host. The principle barrier to reaction is expected to be the expansion of the basal spacing to accommodate the new guest ions. One way in which this barrier can be minimized is via a phenomenon known as staging. This refers to a situation in which some interlayer spaces are completely or partially occupied, while other spaces remain empty. The order of staging is defined as the number of empty layers between successive filled layers. Hence, a second-stage intermediate has alternate layers occupied/unoccupied. Staging is rarer with weak interlayer interactions, and with materials containing rigid layers, such as LDHs.

Fogg et al. discovered that during the intercalation of a variety of carboxylates into h-LiAl−Cl a second-stage

* To whom correspondence should be addressed. Tel.: +44 1865 285130. Fax: +44 1865 285131. E-mail: dermot.ohare@chem.ox.ac.uk.

(1) Yamanaka, S.; Kawaji, H.; Hotehama, K.; Ohashi, M. *Adv. Mater.* **1996**, *8*, 771.
(2) Reichle, W. *J. Catal.* **1985**, *94*, 547.
(3) Cavini, F.; Trifiro, E.; Vaccari, A. *Catal. Today* **1991**, *11*, 173.
(4) Besserguenev, A. V.; Fogg, A. M.; Francis, R. J.; Price, S. J.; O'Hare, D.; Isupov, V. P.; Tolochko, B. P. *Chem. Mater.* **1997**, *9*, 241.
(5) Fogg, A. M.; Freij, A. J.; Parkinson, G. M. *Chem. Mater.* **2002**, *14*, 232.
(6) Lei, L.; Vijayan, R. P.; O'Hare, D. *J. Mater. Chem.* **2001**, *11*, 3276.
(7) Lei, L. X.; Millange, F.; Walton, R. I.; O'Hare, D. *J. Mater. Chem.* **2000**, *10*, 1881.
(8) Millange, F.; Walton, R. I.; Lei, L. X.; O'Hare, D. *Chem. Mater.* **2000**, *12*, 1990.
(9) Chibwe, M.; Valim, J. B.; Jones, W. *NAT ASI Ser., Ser. C* **1993**, (400), 191.
(10) Khan, A. I.; O'Hare, D. *J. Mater. Chem.* **2002**, *12*, 3191.
(11) Rives, V., Ed. *Layered Double Hydroxides: Present and Future*, Nova Scotia Publishers, Inc.: Happauge, NY, 2001.
(12) Auerbach, S. M., Carrado, K. A., Dutta, P. K., Eds. *Handbook of Layered Materials*, Marcel Dekker, Inc.: New York, 2004.

10.1021/cm0503275 CCC: $30.25
Published on Web 04/22/2005

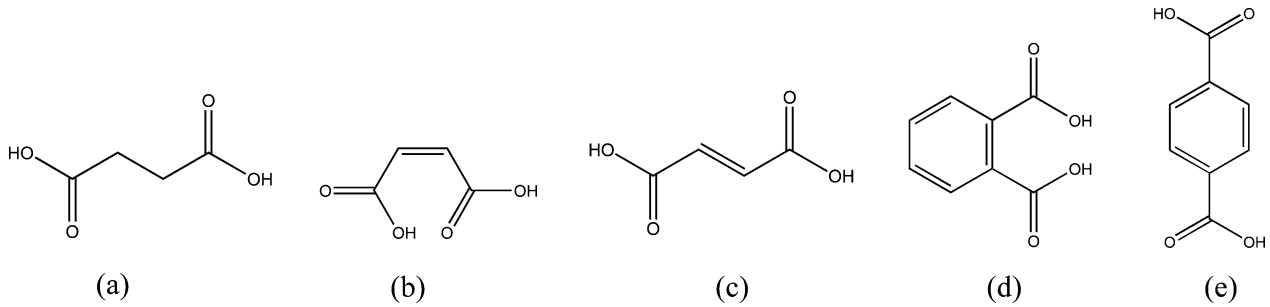

Figure 1. The dicarboxylic acids used in this investigation: (a) succinic, (b) maleic, (c) fumaric, (d) phthalic, and (e) terephthalic acids.

intermediate forms before the final first-stage product.[13] Similar results have been observed for organic phosphonate anions.[14,15] Additionally, Besse et al. have reported staging during the intercalation of succinate and tartrate into $[Zn_2Al(OH)_6]Cl{\cdot}mH_2O$ and $[Zn_2Cr(OH)_6]Cl{\cdot}mH_2O$,[16] and Iyi has reported staging when intercalating (4-phenylazo-phenyl)-acetic acid into a Mg−Al LDH via a coprecipitation route.[17]

To develop a better understanding of these reaction pathways, O'Hare and co-workers have developed an chemical reaction cell which allows the study of intercalation reactions using in situ diffraction methods.[18,19] This approach has two major advantages over conventional quenching experiments. First, the in situ probe is noninvasive, whereas it has been shown that quenched products do not necessarily reflect the reaction matrix at the time of quenching. Second, in situ experiments allow reactions to be continuously monitored, and a much greater amount of detailed structural data can be collected. Time-resolved in situ diffraction methods have previously been used to study the kinetics of a variety of intercalation reactions.[20−23]

Energy-dispersive X-ray diffraction (EDXRD) is extremely suitable for the study of intercalation processes because the simultaneous observation of a wide range of *d* spacings is possible. An energy-discriminating detector is positioned at a fixed angle to a white synchrotron X-ray beam, and the full polychromatic nature of the incident beam is used to simultaneously record a diffraction pattern over a wide range of *d* spacings. Therefore, Bragg reflections are separated by their energy. The detector monitors the number of photons diffracted by the reaction mixture as a function of energy. This is in contrast to angle-dispersive diffraction where the radiation source has a fixed wavelength and a moving detector is used to record diffraction peaks, meaning the Bragg reflections are separated by a spatial coordinate.

As each phase evolves and crystallizes during an intercalation reaction, it will give rise to its own distinct set of Bragg reflections. In principle, it is possible to simultaneously observe host, product, and any crystalline intermediates that may form during these reactions. The diffraction data can be used to quantitatively determine the kinetics and to gain new insight into the mechanisms of these heterogeneous reactions.

The work described in this paper builds on earlier work performed by O'Hare and co-workers.[13−15] The intercalation of a variety of dicarboxylates (Figure 1) and phosphonates (methyl-, ethyl-, phenyl- and benzylphosphonate: MPA, EPA, PPA and BPA, respectively) into both the hexagonal and rhombohedral forms of $[LiAl_2(OH)_6]X{\cdot}mH_2O$ has been investigated for $X = Cl^-$, Br^-, and NO_3^-. The aim of this work was to elucidate exactly how the variation of the layer stacking sequence and the initial interlayer anion affected the intercalation process, and to gain more insight into these complex processes.

Experimental Details

Reagents. Phosphonic and carboxylic acids were purchased from Aldrich or Lancaster and were used as supplied. Carboxylic acids were sourced as the disodium salt if possible. $[LiAl_2(OH)_6]X{\cdot}mH_2O$ was synthesized by reacting $Al(OH)_3$ with a 10-fold excess of LiX at 90 °C for 48 h. The hexagonal material was synthesized using gibbsite as the starting material and the rhombohedral form from a bayerite precursor.

Synthesis. Potassium salts of phosphonic acids were synthesized by creating a solution of the acid at an appropriate pH (using KOH). All reactions were performed at pH 8 unless stated otherwise. If the disodium salt of a carboxylic acid was not available, then it was synthesized from the acid precursor by adding a 5-fold excess of sodium hydroxide to the acid in ethanol. Once the salt precipitated out, it was recovered by vacuum filtration.

First-stage products were synthesized ex situ as follows: 7 mmol of $[LiAl_2(OH)_6]X{\cdot}mH_2O$ was reacted with a 3-fold excess of the phosphonate or dicarboxylate (at pH 8 in the former case). The mixture was stirred for 5 h at room temperature and then the product was isolated by filtration, washed with water and acetone, and dried under vacuum for 1−2 h.

Time-Resolved in Situ Energy-Dispersive X-ray Diffraction (EDXRD) Experiments. Experiments were carried out on Station 16.4 of the UK Synchrotron Radiation Source (SRS) at the Daresbury Laboratory. The SRS operates with an average stored current of 200 mA and a typical beam energy of 2 GeV. A wiggler

(13) Fogg, A. M.; Dunn, J. S.; O'Hare, D. *Chem. Mater.* **1998**, *10*, 356.
(14) Williams, G. R.; Norquist, A. J.; O'Hare, D. *Chem. Commun.* **2003**, 1816.
(15) Williams, G. R.; Norquist, A. J.; O'Hare, D. *Chem. Mater.* **2004**, *16*, 975.
(16) Pisson, J.; Taviot-Gueho, C.; Israeli, Y.; Leroux, F.; Munsch, P.; Itie, J.-P.; Briois, V.; Morel-Desrosiers, N.; Besse, J. P. *J. Phys. Chem. B* **2003**, *107*, 9243.
(17) Iyi, N.; Kurashima, K.; Fujita, T. *Chem. Mater.* **2002**, *14*, 583.
(18) Evans, J. S. O.; Francis, R. J.; O'Hare, D.; Price, S. J.; Clarke, S. M.; Flaherty, J.; Gordon, J.; Nield, A.; Tang, C. C. *Rev. Sci. Instrum.* **1995**, *66*, 2442.
(19) Clark, S. M.; Nield, A.; Rathbone, T.; Flaherty, J.; Tang, C. C.; Evans, J. S. O.; Francis, R. J.; O'Hare, D. *Nucl. Instrum. Methods* **1995**, *97*, 98.
(20) Fogg, A. M.; Green, V. M.; Harvey, H. G.; O'Hare, D. *Adv. Mater.* **1999**, *11*, 1466.
(21) Fogg, A. M.; O'Hare, D. *Chem. Mater.* **1999**, *11*, 1771.
(22) O'Hare, D.; Evans, J. S. O.; Fogg, A.; O'Brien, S. *Polyhedron* **2000**, *19*, 297.
(23) Evans, J. S. O.; Price, S. J.; Wong, H. V.; O'Hare, D. *J. Am. Chem. Soc.* **1998**, *120*, 10837.

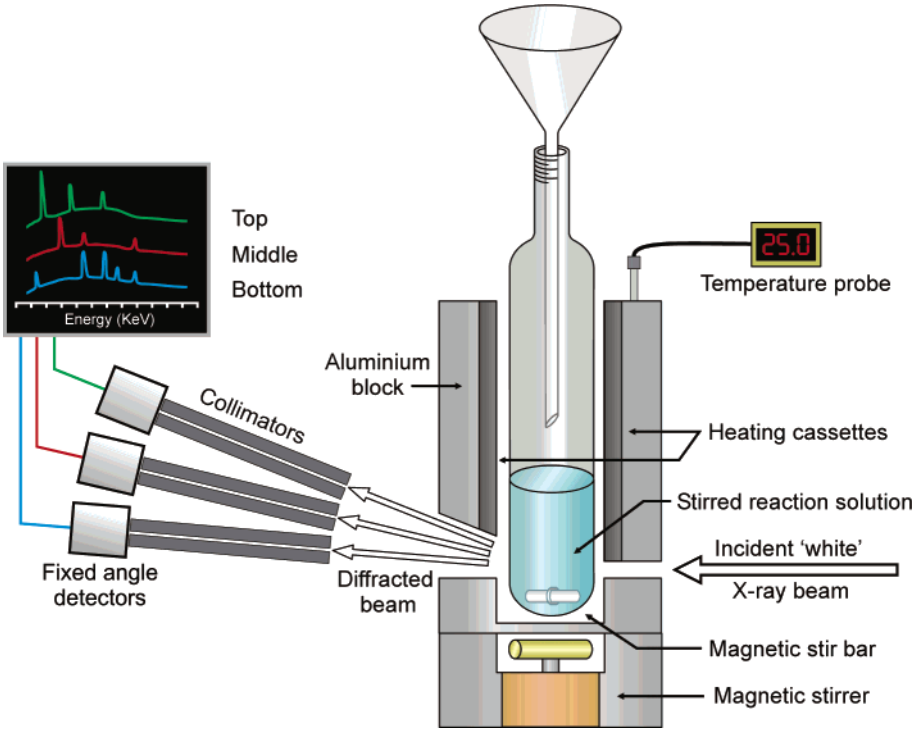

Figure 2. The experimental apparatus used to perform time-resolved in situ EDXRD experiments.

magnet working at a peak field of 6 T supplies Station 16.4 with X-ray frequency radiation. The usable X-ray flux is continuous in the range 5−120 keV, with a maximum flux of 3×10^{10} photons s^{-1} at approximately 13 keV. A three-element detector system is employed. Each detector is separated by approximately 2° in 2θ. and covers a different range of d spacings. Some overlap exists between detectors, ensuring that no Bragg reflections are missed.

Intercalation reactions were performed in glass ampules contained within a temperature-controlled block (Figure 2). Temperatures between room temperature and 250 °C can be accessed using this apparatus (an alternative cell is employed for reactions at lower temperatures).[24] EDXRD spectra were collected at a fixed detector angle of ca. 1.7° in 2θ with an acquisition time of 30 s. The products were filtered, dried, and characterized using X-ray powder diffraction (XPD), elemental analysis (EA), IR spectroscopy, and thermogravimetric analysis (TGA).

In a typical experiment, a 0.19 M solution of the guest species was added at a rate of 0.225 mL min^{-1} to a suspension of 7 mmol of the desired LDH in 10 mL of deionized water, using a SAGE instruments syringe pump. Such slow addition of the guest species to a suspension of the host is necessary owing to the very rapid nature of these reactions.

Data Analysis. An automated Gaussian fitting routine is used to obtain the peak areas of the Bragg reflections.[25] These values are subsequently converted to the extent of reaction at time t, $\alpha(t)$, defined as $\alpha(t) = I_{hkl}(t)/I_{hkl}(\max)$, where $I_{hkl}(t)$ is the area of a given peak at time t and $I_{hkl}(\max)$ is the maximum area of this peak.

Powder X-ray Diffraction. Powder XRD patterns were recorded on a PANalytical X'Pert Pro diffractometer at 40 kV and 40 mA, using Cu Kα radiation.

Infrared Spectroscopy. Infrared experiments were carried out using a Perkin-Elmer 1600 series FTIR spectrometer. Samples were mixed with KBr and made into pellets and spectra were recorded between 4000 and 400 cm^{-1}; 32 scans were recorded with a scan resolution of 4 cm^{-1}.

Thermogravimetric Analysis. TGA measurements were performed on a Rheometric Scientific STA-1500H instrument. Approximately 20 mg of sample was heated in a platinum crucible between 25 and 800 °C at a heating rate of 10 °C/min under a stream of argon.

Results

Even for what appears to be a very simple reaction such as the ion-exchange intercalation of LDHs, we have observed that both the final isolated product and the precise course of the reaction may be influenced by a number of subtle factors. In some cases the final product is affected by the deintercalating anions, while the observation of second-stage intermediate phases during the reaction is dependent on a number of factors, for example, the chemical composition of the host, the layer stacking sequence of the host, the intercalating ions, and the identity of the deintercalating anion. In the follow section we try to unravel the role of these variables in the case of the intercalation of some organic anions into a series of LiAl−X LDHs.

Products Formed. The final products formed by the anion exchange of carboxylates into the LiAl−X materials are found to be almost invariant with respect to the layer stacking sequence and starting interlayer anion. The idealized formula of the intercalate phase is $[LiAl_2(OH)_6](A)_{0.5}\cdot mH_2O$, where A^{2-} represents any dianionic carboxylate ion. Previous work by Fogg[5,13] has investigated some carboxylate intercalates of both the hexagonal and rhombohedral forms of LiAl−Cl (h-LiAl−Cl and r-LiAl−Cl, respectively). The resulting compounds were found to be practically identical in terms of interlayer separation and elemental composition.

In contrast, there is some influence of the initial interlayer anion on the product of the phosphonate intercalation

(24) Neild, A. A.; Hammond, W. B.; Abram, D.; Bates, A.; Wilkinson, P. J.; Taylor, D. J. Manuscript in preparation.
(25) Clark, S. M. *J. Appl. Crystallogr.* **1995**, *28*, 646.

Table 1. Phosphonate Intercalates of Hexagonal and Rhombohedral LiAl−X, Where X = Br^- and NO_3^-

host LDH	phosphonate	*d*-spacing/Å	formula of intercalate
h-LiAl−Br	MPA	12.7 (wet)	
		11.0 (dry)	$[Li_{0.7}Al_2(OH)_6](MePO_3)_{0.3}(MePO_3H)_{0.1}{\cdot}3.2\ H_2O$
	EPA	13.4	$[Li_{0.74}Al_2(OH)_6](EtPO_3)_{0.37}{\cdot}2.7H_2O$
	PPA	15.4	$[Li_{0.79}Al_2(OH)_6](PhPO_3)_{0.30}(PhPO_3H)_{0.19}{\cdot}3.2H_2O$
	BPA	15.9	$[Li_{0.77}Al_2(OH)_6](PhCH_2PO_3)_{0.3}(PhCH_2PO_3H)_{0.17}{\cdot}2.7H_2O$
h-LiAl−NO3	MPA	12.7 (wet)	
		11.0 (dry)	$[Li_{0.68}Al_2(OH)_6](MePO_3)_{0.34}{\cdot}2.4H_2O$
	EPA	13.6	$[Li_{0.72}Al_2(OH)_6](EtPO_3)_{0.36}{\cdot}2.5H_2O$
	PPA	15.6	$[Li_{0.74}Al_2(OH)_6](PhPO_3)_{0.28}(PhPO_3H)_{0.18}{\cdot}2.3H_2O$
	BPA	16.2	$[Li_{0.84}Al_2(OH)_6](PhCH_2PO_3)_{0.25}(PhCH_2PO_3H)_{0.34}{\cdot}2.4H_2O$
r-LiAl−Cl	MPA	12.7 (wet)	
		11.4 (dry)	$[Li_{0.8}Al_2(OH)_6](MePO_3)_{0.35}(MePO_3H)_{0.1}{\cdot}3.2H_2O$
	EPA	13.5	$[Li_{0.85}Al_2(OH)_6](EtPO_3)_{0.35}(EtPO_3H)_{0.15}{\cdot}2.6H_2O$
	PPA	15.7	$[Li_{0.92}Al_2(OH)_6](PhPO_3)_{0.3}(PhPO_3H)_{0.32}{\cdot}2H_2O$
	BPA	16.7	$[Li_{0.94}Al_2(OH)_6](PhCH_2PO_3)_{0.2}(PhCH_2PO_3H)_{0.54}{\cdot}3H_2O$
r-LiAl−NO3	MPA	12.7 (wet)	
		11.0 (dry)	$[Li_{0.48}Al_2(OH)_6](MePO_3)_{0.24}{\cdot}1.8H_2O$
	EPA	13.2	$[Li_{0.6}Al_2(OH)_6](EtPO_3)_{0.25}(EtPO_3H)_{0.1}{\cdot}2.5H_2O$
	PPA	15.3, 14.0	$[Li_{0.59}Al_2(OH)_6](PhPO_3)_{0.2}(PhPO_3H)_{0.19}{\cdot}2.7H_2O$
	BPA	16.3	$[Li_{0.55}Al_2(OH)_6](PhCH_2PO_3)_{0.2}(PhCH_2PO_3H)_{0.15}{\cdot}1.8H_2O$
r-LiAl−Br	MPA	12.7 (wet)	
		11.0 (dry)	$[Li_{0.88}Al_2(OH)_6](MePO_3)_{0.26}\,(MePO_3H)_{0.26}Br_{0.1}{\cdot}3.8H_2O$
	EPA	13.5	$[Li_{0.78}Al_2(OH)_6](EtPO_3)_{0.39}{\cdot}2.4H_2O$
	PPA	15.3	$[Li_{0.89}Al_2(OH)_6](PhPO_3)_{0.36}(PhPO_3H)_{0.17}{\cdot}2.3H_2O$
	BPA	15.8	$[Li_{0.78}Al_2(OH)_6](PhCH_2PO_3)_{0.3}(PhCH_2PO_3H)_{0.18}{\cdot}2.4H_2O$

reactions. Elemental analysis and powder X-ray diffraction data for these materials are given in Table 1. The PXRD pattern for the PPA intercalation compound is presented in Figure 3. Thermogravimetric analysis has additionally been used to confirm the formulas suggested, and to investigate the nature of the decomposition product. IR spectroscopy has been used to demonstrate that the reaction product contains intact phosphonate anions. For the PPA reaction product, O−H vibrations occur at ca. 3500 cm^{-1}, the δ-vibrations of H_2O are seen at approximately 1640 cm^{-1}, and the distinctive P−C stretch is observed at 1438 cm^{-1}. There are additionally a number of vibrations corresponding to the C−PO_3 group between 1150 and 1000 cm^{-1} and vibrations of the layers seen below 1000 cm^{-1}.

Hence, the initial interlayer anion, which is deintercalating during the course of the reaction, plays a role in determining the ratio of mono- and divalent anions intercalated, and therefore the interlayer spacing. However, these differences are fairly small, and no unambiguous trend can be extracted from the available data.

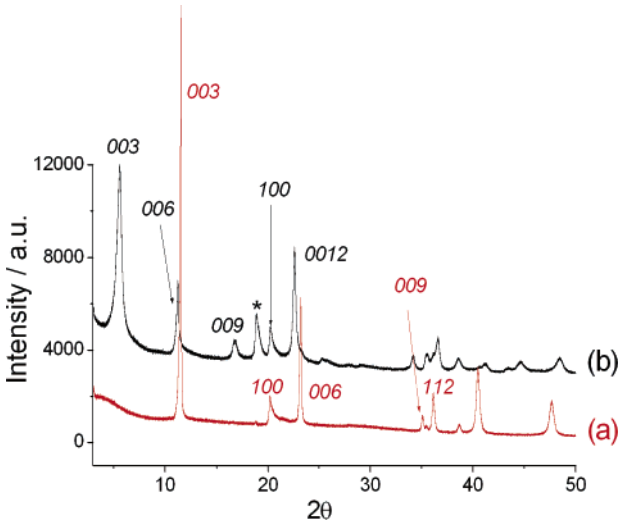

Figure 3. X-ray powder diffraction pattern for (a) r-LiAl−Cl and (b) the reaction product of r-LiAl−Cl and PPA. The peak in (b) marked with a * denotes bayerite ($Al(OH)_3$) which forms concomitantly with the intercalation process.

Effect of the Layer Stacking Sequence on Reaction Mechanism. *(i) The Hexagonal System.* Previous work by O'Hare and co-workers has successfully observed second-stage intermediates during the intercalation of a wide variety of carboxylates (including those which form the focus of this study) into the hexagonal form of $[LiAl_2(OH)_6]Cl{\cdot}H_2O$ (h-LiAl−Cl).[13] Analogous intermediate phases have also previously been observed for the intercalation of methyl and benzylphosphonates (MPA and BPA) into h-LiAl−Cl.[14,15] However, no intermediates were observed for ethyl or phenylphosphonate (EPA and PPA). The rate of intercalation of PPA is much slower than the rate of intercalation of the other phosphonates, so in this case the absence of observable intermediates may be due to the higher activation energy of this reaction (staging is never observed for intercalation reactions requiring elevated temperatures: see Discussion). However, it was very surprising that no intermediate was observed for EPA, and so a number of further experiments were performed to see if there genuinely is no intermediate, or whether an intermediate formed but was missed in the initial experiment owing to poor resolution of the energy-dispersive detector.

After a number of attempts, improvements to the detector system in operation at the experimental station allowed the observation of a second-stage intermediate for the EPA system. This is consistent with the results previously obtained: data are given in Figure 4. Note that the host and second-stage α vs time curves cross at ca. $\alpha = 0.5$. This suggests a direct transformation from the host to the intermediate; loss of coherency of the host diffraction is matched by the gain in intensity of the intermediate reflection. In contrast, the second-stage intermediate and first-stage

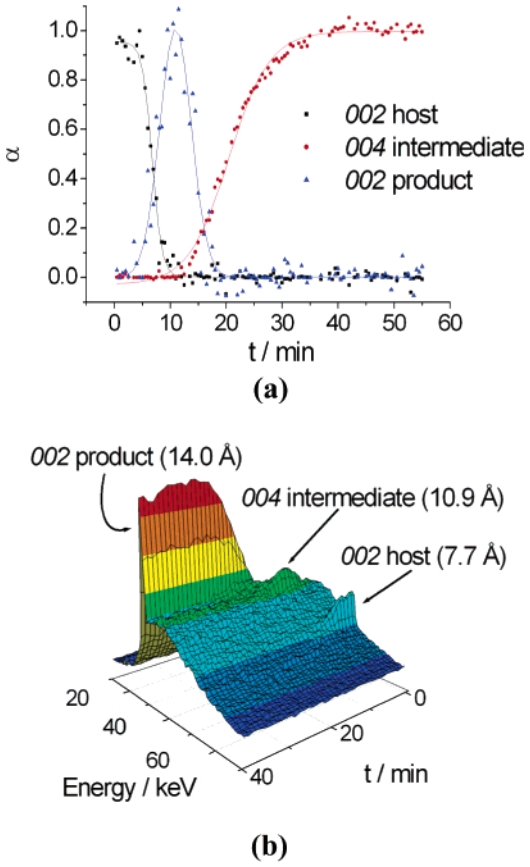

Figure 4. EDXRD data for the intercalation of EPA into h-LiAl−Cl. (a) The evolution of the host *002*, intermediate *004* and and product *002* reflections. (b) 3D stacked plot showing the same.

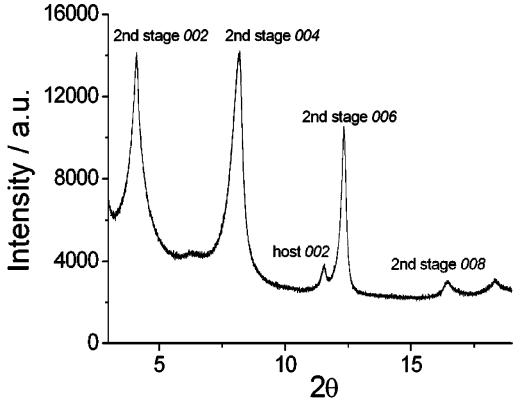

Figure 5. X-ray powder diffraction pattern showing the presence of host and second-stage product isolated during the intercalation path of EPA into h-LiAl−Cl.

product curves cross at $\alpha < 0.5$. This arises as a result of random filling of the Cl-containing layers after alternate layers have been filled with EPA.

The nature of the intermediate has been confirmed by quenching the reaction where the concentration of intermediate is expected to be greatest. X-ray powder diffraction (XPD), elemental analysis (EA), IR spectroscopy, and thermogravimetric analysis (TGA) have been used to characterize the solid produced from the quenching experiment. The material is not phase pure, but consists of a mixture of the product and the intermediate. The XPD pattern (Figure 5) contains Bragg reflections at *d* spacing 21.5 Å (second-stage intermediate *002*), 10.8 Å (second-stage *004*), and 7.7 Å (host *002*). The second-stage material has alternate layers occupied by chloride and EPA, and hence has a predicted $d_{002} = d_{002}(\text{host}) + d_{002}(\text{first-stage product}) = 7.7 + 13.8 = 21.5$ Å. Analysis of EA results gives the formula $[Li_{0.8}Al_2(OH)_6](EtPO_3H)_{0.45}Cl_{0.41}\cdot 2H_2O$. Percentages obsd. (calcd.): Li 2.14 (2.29), Al 20.21 (20.66), P 4.87 (5.33), C 4.52 (4.14), H 5.09 (4.73), Cl 5.94 (5.57). TGA measurements (Figure 6) confirm this assignation. Mass loss occurs in three stages, corresponding to the loss of interlayer water, dehydration of the layers, and partial decomposition of the guest anions (see Figure 6). The bands observed in the IR spectrum confirm the presence of intact EPA anions in the isolated material.

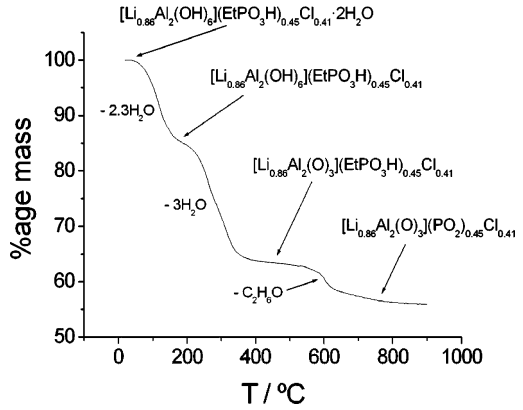

Figure 6. Thermogravimetric analysis data for material isolated from quenching the intercalation of EPA into h-LiAl−Cl at pH 8.

(ii) The Rhombohedral System. Organic dicarboxylates have also been intercalated into the rhombohedral form of LiAl−Cl (r-LiAl−Cl).[5] We were interested to see if the kinetics and the mechanism of these reactions were similar to the analogous reactions with the hexagonal polytype discussed earlier. Time-resolved, in situ EDXRD experiments were performed on the intercalation of succinate, fumarate, maleate, terephthalate, and phthalate into r-LiAl−Cl. In all five cases, the reaction was observed to proceed directly from the host material to the product—no staging intermediates were seen. The ion-exchange intercalation of the phthalate anion into r-LiAl−Cl is shown in Figure 7. The extent of reaction (α) vs time curves of the host and the product are seen to cross at $\alpha \approx 0.5$. This is consistent with a direct conversion of host to product; if intermediates were seen, then the host and product curves are expected to cross at almost zero.

Another series of in situ EDXRD experiments were performed to follow the rate of intercalation of the phosphonate anions MPA, EPA, PPA, and BPA into r-LiAl−Cl. Again, these reactions were observed to be one-step processes, proceeding directly from the host to the product. In no case could any Bragg reflections due to intermediate phases be observed. The in situ EDXRD data for intercalation of MPA intercalation at pH 8 are presented in Figure 8; the extent of reaction (α) vs time curves cross close to $\alpha \approx 0.5$.

In the case of h-LiAl−Cl, it was possible to extract kinetic parameters for the phosphonate intercalation reactions by performing experiments at low temperatures with $T < 10$ °C (this is not possible for carboxylates: even at very low temperatures the reactions are observed to be complete in a

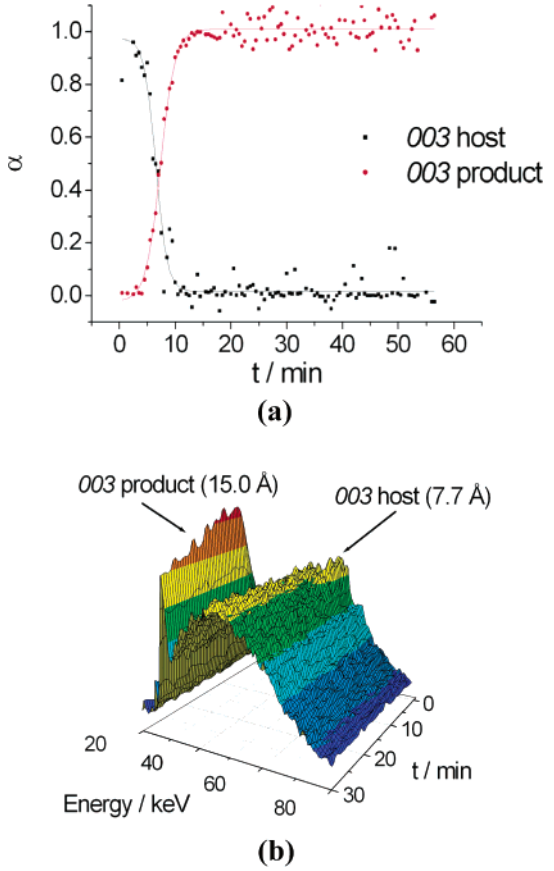

Figure 7. EDXRD data showing the intercalation ofphthalate into r-LiAl−Cl: (a) plot showing the evolution of host (003) Bragg reflection and product (003) reflection with time; (b) 3D stacked plot showing the same.

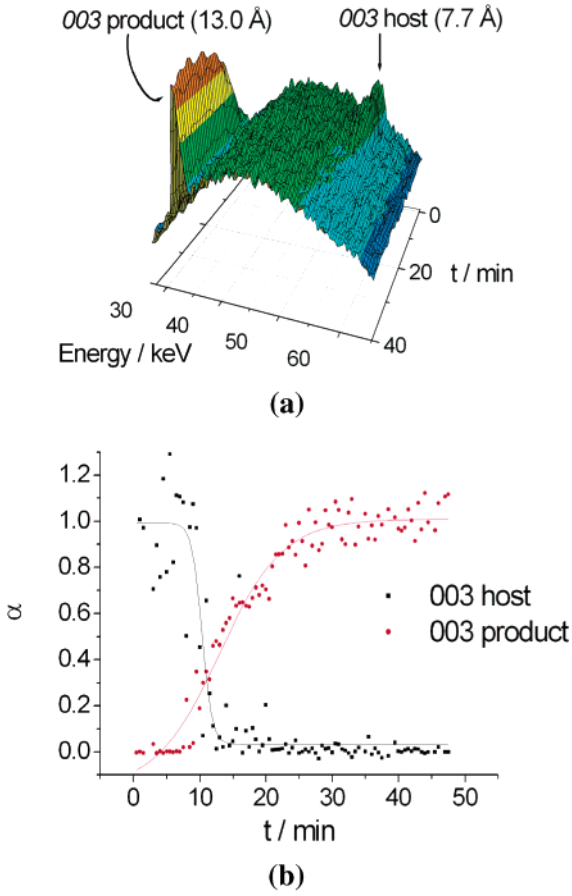

Figure 8. EDXRD data showing the intercalation of MPA into r-LiAl−Cl: (a) plot showing the evolution of host (003) and product (003) reflections with time; (b) 3D stacked plot.

few minutes). For r-LiAl−Cl, the reactions are much faster than for the hexagonal analogue. Therefore, it proved impossible to collect much kinetic data using our current in situ EDXRD apparatus. However, performing the intercalation of PPA in r-LiAl−Cl at 4.4 °C allowed us to measure a limited number of kinetic parameters. We determined the value of the Avrami exponent[26−28] to be 0.56, which indicates that the reaction is entirely diffusion-controlled, and nucleation plays no part in determining the rate of reaction. This is consistent with the observation that at RT these reactions reach completion in a few minutes. The rate constant, *k*, was found to be 4.5×10^{-3} s^{-1}. This is an order of magnitude greater than the values found with the h-LiAl−Cl system, where the rate of ion exchange of PPA at 3.8 °C was 0.33×10^{-3} s^{-1}. This very great difference in rates probably explains the lack of staging intermediates observed for the rhombohedral system (see Discussion).

Effect of the Initial Interlayer Anion on Reaction Mechanism. *(i) Nitrate Systems.* It is clear from the above discussion that the layer stacking sequence in the LDH is of paramount importance in determining whether the intercalation of carboxylates and phosphonates is a direct, one-step process or whether an intermediate phase is involved. Therefore, a second series of experiments was performed to determine what effect the initial interlayer anion had on the reaction. The affinity of LDHs for various anions has previously been extensively investigated.[29−33] The intercalation reactions of the carboxylate and phosphonate ions discussed above into both the hexagonal and rhombohedral forms of $[LiAl_2(OH)_6]X{\cdot}mH_2O$, where X = Br and NO_3 (h-LiAl−Br, r-LiAl−Br, h-LiAl−NO_3, and r-LiAl−NO_3) were studied using in situ EDXRD.

The h-LiAl−NO_3 and r-LiAl−NO_3 materials showed no evidence for staging intermediates in the anion-exchange reactions with any of the carboxylates or phosphonates. Plots showing the time evolution of the reactions with MPA at pH 8 are presented in Figure 9. The crossing of the extent of reaction (α) vs time curves at $\alpha \approx 0.5$ confirms these processes to be direct conversions from the host to the product. It is thought that the lack of staging in these systems is a result of the ease of replacement of nitrate (see Discussion).

(ii) Bromide Systems. The results from the series of experiments involving h-LiAl−Br and r-LiAl−Br were much more interesting than those from the nitrate system. For h-LiAl−Br, no staging was observed for intercalation of phthalate, nor for BPA or PPA. The extent of reaction (α) vs time curves of the host and product are observed to cross

(26) Avrami, M. *J. Phys. Chem.* **1940**, *8*, 212.
(27) Avrami, M. *J. Phys. Chem.* **1941**, *9*, 177.
(28) Erofe'ev, B. V.; Dokl, C. R. *Acad. Sci. USSR* **1946**, *52*, 511.
(29) Miyata, S. *Clays Clay Miner.* **1975**, *23*, 369.
(30) Miyata, S. *Clays Clay Miner.* **1980**, *28*, 50.
(31) Miyata, S. *Clays Clay Miner.* **1983**, *31*, 305.
(32) Miyata, S.; Kumura, T. *Chem. Lett.* **1975**, 843.
(33) Miyata, S.; Okada, A. *Clays Clay Miner.* **1977**, *25*, 14.

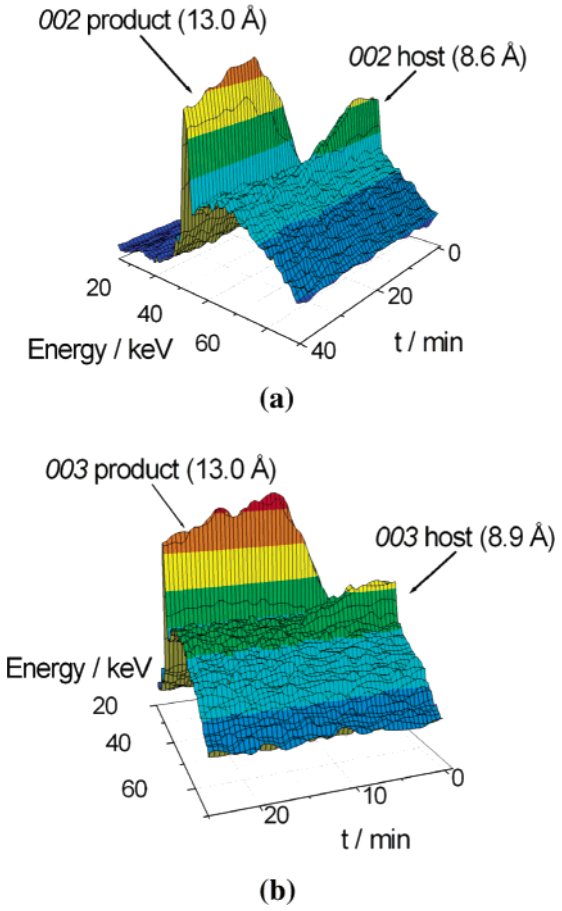

Figure 9. The intercalation of MPA into (a) h-LiAl−NO_3 and (b) r-LiAl−NO_3 at pH 8, as observed using time-resolved EDXRD.

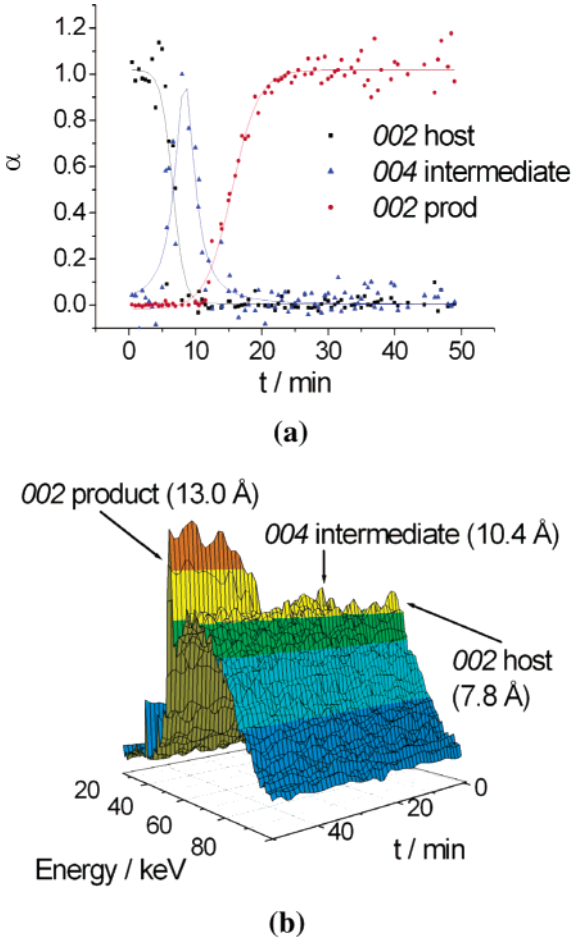

Figure 10. The intercalation of MPA into h-LiAl−Br at pH 8. (a) 2D plot showing the host (002), intermediate (004), and product (002) reflections and (b) 3D plot in which the same reflections may be observed.

at $\alpha \approx 0.5$. However, a crystalline intermediate phase is observed during MPA intercalation at pH 8 (Figure 10). This intermediate was initially very hard to observe; only the fact that the extent of reaction (α) vs time curves crossed at $\alpha \approx 0$ suggested an intermediate, and it took significant painstaking analysis of the data to spot the poorly crystalline intermediate phase that was present. Quenching the reaction where the concentration of the intermediate is expected to be greatest allowed the isolation of a non phase pure sample containing both the starting material and the intermediate. Characterization of this material by EA, TGA, IR, and XPD confirmed it to be a second-stage intermediate with $d_{002} = 20.8$ Å and $d_{004} = 10.4$ Å.

For the intercalation of EPA, succinate, fumarate, maleate, and terephthalate into h-LiAl−Br, second-stage intermediate phases are also observed. Again, the crystallinity of these tends to be rather poor, which makes detection difficult, although once detected these phases can be assigned to be second-stage intercalates with a high degree of confidence.

In the case of r-LiAl−Br, the results are again interesting. The intercalation of maleate, phthalate, terephthalate, EPA, BPA, and PPA in r-LiAl−Br is observed to proceed in a one-step process, directly from the host to the product, again with the α−time curves intersecting at ca. 0.5. The intercalation of MPA at pH 8 proceeds differently, however (Figure 11). From the 2D plot, it is clear that the Bragg reflections of the host decay away while initially no new Bragg reflections grow in intensity. The α vs time curves cross at $\alpha \approx 0$. It is not possible to resolve any intermediate reflections during this process. If this reaction is quenched halfway between the disappearance of the host reflection and the emergence of the product reflection, then a material with the XPD pattern given in Figure 12 is isolated. The assignments of the Bragg reflections depicted in Figure 12 are presented in Table 2.

From Figure 12 and Table 2, it is possible to see that the isolated material contains three phases: the host, the product, and an intermediate phase. The intermediate is identified as being a second-stage intermediate, with $d_{003} = 20.8$ Å. The failure to observe the intermediate phase in situ can be attributed to a combination of two factors: the poor crystallinity of the intermediate phase and also the relatively poor resolution of the EDXRD detector. Note that, in previous cases where no intermediates are seen, this is not simply because they are too poorly crystalline and cannot be resolved, but because they do not exist. This has been unequivocally determined from the α vs time curve intersections and using quenching studies.

Therefore, it can be seen that the intercalation of MPA into r-LiAl−Br proceeds via a second-stage intermediate. Similarly, for the intercalation of succinate and fumarate poorly crystalline second-stage intermediates lie on the reaction coordinate prior to the formation of the product.

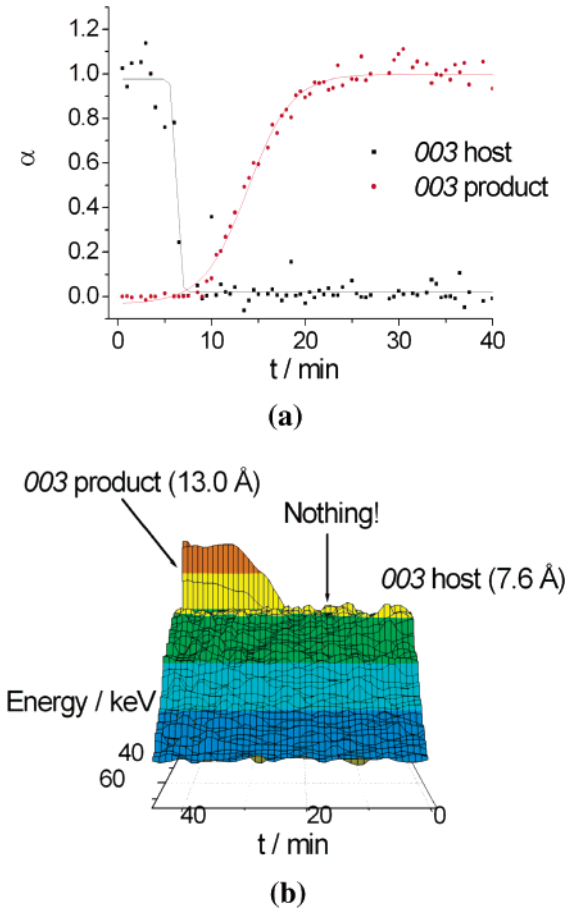

Figure 11. The intercalation of MPA into r-LiAl−Br at pH 8. (a) 2D plot showing the host and product (003) reflections and (b) 3D plot in which the same reflections may be observed.

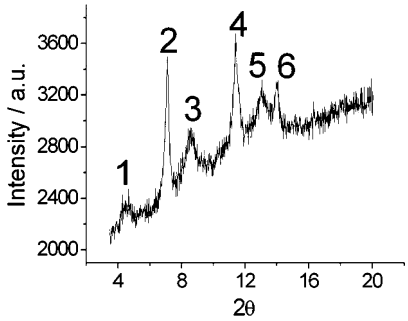

Figure 12. XPD pattern for the material isolated when quenching the intercalation of MPA into r-LiAl−Br at pH 8.

Table 2. Assignments of the Bragg Reflections Shown in Figure 12

no.	*d*-spacing	index
1	20.8	second-stage *003*
2	12.6	first-stage *003*
3	10.4	second-stage *006*
4	7.7	host *003*
5	6.8	second-stage *009*
6	6.3	first-stage *006*

Discussion

The data presented above show that the stacking sequence of the layers (*aba* or *abca*) and the nature of the initial interlayer anion are vital in determining whether the intercalation of carboxylates and phosphonates into a series of crystalline layered double hydroxides occurs in a one-step or a two-step process. A number of trends may be identified. First, staging is never seen for intercalation of PPA. The reaction of PPA with h-LiAl−Cl is observed to be relatively slow in comparison to the reaction rates of the other phosphonates and carboxylates. From the considerable body of data known so far, it seems that staging is only observed with very fast reactions (i.e., reactions complete within a few minutes at room temperature). In contrast, PPA intercalates into h-LiAl−Cl gradually over about 30 min at room temperature. Therefore, the failure to observe staging for PPA is consistent with previous data: for slowly intercalating species such as sulfonates and large biological molecules, no staging is observed.

Staging is a way of reducing the energy barrier to intercalation. For slow reactions, the energy barrier will be high since E_a is related to k through the Arrhenius equation. The amount by which staging will reduce this barrier is unknown, but it is likely that if the interactions between the LDH layers and the initial anion are very strong compared to the interactions between the layers and the replacing anion, only a small (maybe negligible) reduction in E_a could be achieved through staging. Hence, reactions such as those with PPA with high E_a proceed slowly in a one-step process rather than exhibiting staging.

Second, staging is observed for all other phosphonates and carboxylates for h-LiAl−Cl, yet no staging is seen for r-LiAl−Cl. Staging is also not observed for intercalation into h-LiAl−NO_3 or r-LiAl−NO_3. In the case of h-LiAl−Br, staging is seen for MPA, EPA, succinate, fumarate, maleate, and terephthalate and for r-LiAl−Br for MPA, succinate, and fumarate. Some clear trends can be seen in these data by considering the affinity of the layers for different anions. The order of difficulty of exchange for some common inorganic anions is given below (eq 1).[30,31,33]

$$CO_3^{2-} \gg SO_4^{2-} > OH^- > F^- > Cl^- > Br^- > NO_3^- > I^- \quad (1)$$

Considering first the hexagonal system, a clear correlation can be seen between the occurrence of a two-step process and the difficulty of exchange of the initial anion. Chloride is relatively difficult to replace, and so staging occurs in order to lower the E_a. Bromide is easier to replace, and hence staging is only seen in certain instances. Nitrate is easier still to replace, and so the reaction occurs in one stage owing to the very low value of E_a.

Things are less clear-cut when considering the rhombohedral system: the occurrence of staging does not directly correlate with the ease of exchange of the initial anion. The r-LiAl−Cl system does not exhibit staging, whereas in contrast h-LiAl−Cl does. However, this is understandable if the significantly faster reaction rate of the rhombohedral system is taken into account. Since the r-LiAl−Cl system reacts much more quickly than the hexagonal analogue, the E_a for intercalation into the former system must be significantly lower. Hence, the reaction proceeds in a one step process—staging is not needed to help overcome the small energy barrier to reaction. The difference in reactivity between the rhombohedral and hexagonal forms of the LDH may be ascribed to the fact that layer slippage will be easier in the former case. The r-LiAl−NO_3 system also does not

exhibit staging. Nitrate is easier to replace than chloride, and so staging is not seen here either. These results are all consistent.

The r-LiAl−Br results seem to lie out of line, however. Staging is seen when intercalating MPA, succinate, and fumarate. This is suspected to be a result of size and solvation effects. It is observed that the rate of intercalation of BPA into h-LiAl−Cl is greater than that of MPA and EPA.[14,15] Hence, the fact that for both h-LiAl−Br and r-LiAl−Br the larger BPA and phthalate (and terephthlate for r-LiAl−Br) anions do not show staging might be attributed to the lower activation energy for these reactions. This is likely to be owing to the relatively weak solvation of these anions. If solvation is the principal factor, then the lack of staging with maleate for r-LiAl−Br can also be rationalized with this argument—the cis conformation of maleate means it is much less efficiently solvated than fumarate.

The solvation of the initial guest anion once it has been released from the host matrix is also a factor needing consideration. The small nitrate and chloride anions will be strongly solvated, but the larger bromide anions will be more weakly solvated. Therefore, the occurrence of staging can possibly be explained by a combination of these factors. In the bromide systems, the strong solvation of MPA, succinate, and fumarate (and EPA, maleate, and terephthalate in the hexagonal case) coupled with the weak solvation of the bromide anions being released may cause a relatively high E_a, and thus staging occurs to minimize this barrier. It seems that EPA, maleate and terephthalate are on the borderline for staging, and possibly there are stronger interactions between the layers and the Br anions in the hexagonal case, leading to staging with these anions, whereas this is not seen for the r-LiAl−Br system.

Intercalation reactions are enormously complicated processes. A number of factors operate to determine the kinetics and mechanisms of these reactions, including the interactions between both the initial and final anions and the layers, and the solvation of both anions. These processes are still not well understood, although work is ongoing in this area. There is a suggestion that staging occurs as a result of a hydrophobic/hydrophilic separation.[16,34] This is consistent with the results presented here, and other results achieved recently, where staging is only seen with organic anions. However, it should be noted that staging is not seen with all organic anions, and it seems that the models we have to describe these processes are at the moment overly simple. Work is ongoing to increase the number of systems studied and further our understanding of these fascinating processes.

Acknowledgment. The authors would like to thank the EPSRC and St. Hugh's College, Oxford, for funding, and they gratefully acknowledge the help of Dr. A. Norquist, and also Dr. D. Taylor and Mr. A. Neild at the Daresbury Laboratory.

CM0503275

(34) Taviot-Gueho, C.; Leroux, F.; Payen, C.; Besse, J. P. *Appl. Clay Sci.* **2005**, *28*, 111.